International Journal of Solids and Structures 48 (2011) 1210–1218

Contents lists available at ScienceDirect

International Journal of Solids and Structures

journal homepage: www.elsevier.com/locate/ijsolstr

Cracked elastic layer under compressive mechanical loads

V. Makaryan [a], M. Sutton [b], D. Hasanyan [b,*], X. Deng [b]

[a] Institute of Mechanics National Academy of Science of Armenia, Yerevan, Armenia
[b] Department of Mechanical Engineering, University of South Carolina, Columbia, SC, USA

ARTICLE INFO

Article history:
Received 22 July 2010
Received in revised form 26 October 2010
Available online 11 January 2011

Keywords:
Elastic layer
Crack
Compressive loading
Contact
Singular integral equation
Orthogonal polynomials
Stress intensity factor

ABSTRACT

We consider boundary value problem in which an elastic layer containing a finite length crack is under compressive loading. The crack is parallel to the layer surfaces and the contact between crack surfaces are either frictionless or with adhesive friction or Coulomb friction.

Based on fourier integral transformation techniques the solution of the formulated problems is reduced to the solution of a singular integral equation, then, using Chebyshev's orthogonal polynomials, to an infinite system of linear algebraic equations. The regularity of these equations is established. The expressions for stress and displacement components in the elastic layer are presented. Based on the developed analytical algorithm, extensive numerical investigations have been conducted.

The results of these investigations are illustrated graphically, exposing some novel qualitative and quantitative knowledge about the stress field in the cracked layer and their dependence on geometric and applied loading parameters. It can be seen from this study that the crack tip stress field has a mode II type singularity.

1. Introduction

Stress concentration is often a critical concern because it affects the durability and reliability of structures and their components. Stress concentrators in structures can exist as a result of material composition imperfections (cavities, inclusions) or they can be caused by technological and structural needs (holes, cuts, etc.). In either case, analyzing the effects of stress concentrators is very important.

Stress concentrators in the form of cracks have been intensively studied in the literature. Since experimental observations indicate that crack growth is often in the form of opening mode crack growth instead of mixed mode or pure shear mode crack growth, the research reported in the literature on the subject of crack growth has mainly focused on mode I fracture (e.g. Erdogan and Sih, 1963; Sih, 1974; Bilby and Cardew, 1975; Cotterell and Rice, 1980; Hayashi and Nemat-Nasser, 1981; or Broberg, 1987).

In the majority of works in the literature it is assumed that the crack surfaces are not in contact. However crack surface contact can occur under compressive loading and such cracks can pose a potential risk just as cracks under tensile loading (e.g. Roy et al., 1999; Deng, 1993, 1995; Dhirendra and Narasimhan, 1998; Ghonem and Kalousek, 1988; Hallbfack, 1998; Hayashi and Nemat-Nasser, 1981; Hearle and Johnson, 1985; Isaksson and Stahle, 2002, 2003; Ishida and Abe, 1996; Hancock, 1999; Makaryan, 2006; Makaryan et al., 2009; Melin, 1986). Due to the elimination of crack surface opening, the growth of cracks with crack surface contact is in the shear mode (or mode II under in-plane loading conditions).

El-Borgi et al. (2004) considered the problem of a functionally graded coating bonded to a semi-infinite homogeneous medium with a crack embedded in the FGM layer and parallel to the free surface. The composite medium is subjected to a frictional Hertzian contact traction loading applied to the surface of the graded coating. The author's utilize a crack closure algorithm whenever the mode I stress intensity factors turn out to be negative under the action of compressive loads.

Broberg (1987) reported laboratory produced mode II crack growth in plates in experiments conducted in a combination of pressure and shear loads. Hearle and Johnson (1985) achieved shear crack growth in experiments performed on rail steels subjected to a moving point load. Ishida and Abe (1996) carried out rolling contact tests in a rail/wheel contact fatigue testing machine and reported sub-surface crack growth in mode II. More recently, the propagation of cracks parallel with a shear loaded surface (which are sub-surface horizontal cracks) due to surface traction caused by contact, have been analytically and numerically investigated by several researchers (e.g. Wong et al., 1996; Jayaraman et al., 1997, Komvopoulos and Cho, 1997). Melin (1987) concluded that mode II crack growth in an elastic material would be preferred over mode I only if the ratio between the critical stress intensity factors K_{IIc} and K_{Ic} is fairly low. The effect of crack surface friction

* Corresponding author. Tel.: +1 757 239 0796.
E-mail address: davreshh@yahoo.com (D. Hasanyan).

0020-7683/$ - see front matter © 2011 Elsevier Ltd. All rights reserved.
doi:10.1016/j.ijsolstr.2011.01.004

on mode II stress intensity factor of a central slant crack in a plate uniformly loaded in uniaxial compression is discussed by Hammouda et al. (2002). Comparison of predictions by mode II or mode III criteria on crack front twisting in three or four point bending experiments was done by Lazarus et al. (2008).

Problems with cracks under compressive forces can be interpreted as problems with contact of two separate bodies pressed against each other (El-Borgi et al., 2006; Keer et al., 1972). In these problems, the length of the contact zone and the contact pressure (which is zero at the ends of the contact segment) are the primary unknowns of the problem.

Practical applications where mode II crack propagation generally is predicted to prevail are in various applications subjected to a load combination of a shear stress and a high compressive normal stress (e.g. gear drives, rolling bearings, railway applications or structures exposed to earth quakes). However, despite the great number of investigations, the phenomena of crack initiation and propagation associated with compressive forces are still not fully understood.

The large number of available investigations in the literature (e.g. Broberg (1999), Civelek and Erdogan (1974), Hill (1950), Hutchinson (1968), Isaksson and Stahle (2002), Liu (1974), Sih et al. (1966), Sundara Raja Iyengar et al. (1988)) has been mainly restricted to the non-interacting crack surfaces (i.e. non-contacting crack surfaces).

In this paper we show that if an elastic layer containing a crack parallel to the layer boundary surfaces is under compressive loading on the layer boundary surfaces the shear stress can became infinite at the crack tips and at the same time the normal stress is finite along the crack line. In other words we show that compressive loading normal to the crack surfaces can lead to a mode II type stress singularity at the crack tips and can initiate mode II type crack growth. To that end, the plane problem of an elastic layer, weakened by a finite-length crack under compressive loading is considered, in which the crack surfaces are in full contact with either no friction or with Coulomb friction or a friction given in advance (i.e. adhesive friction).

Based on the Fourier integral transformation techniques the solution of the formulated problem is reduced to the solution of a singular integral equation, and then, using the Chebyshev's orthogonal polynomials, to an infinite system of linear algebraic equations. The regularity of these equations is established. These equations are solved numerically for several typical cases and the resulting stress distributions are described.

2. Problem description and formulation

Let us suppose that an elastic layer occupies the domain $-\infty < x < \infty$, $-h_1 \leqslant y \leqslant h_2$ and a finite crack $-x_0 < x < x_0$ is located at $y = 0$ (see Fig. 1). The layer surfaces $y = h_1$ and $y = -h_2$ are under the action of certain compressive mechanical forces as shown in Fig. 1., and the crack surfaces are pressed together so that they are in full contact. In other words along the crack surfaces the normal stress satisfy the condition $\sigma_y(x,\pm 0) < 0$.

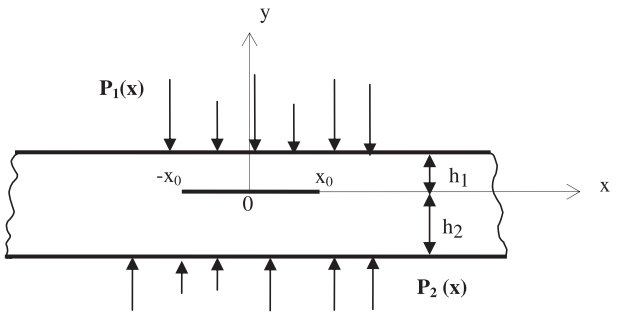

Fig. 1. An elastic layer weakened by a finite length crack and is under the action of compressive surface forces.

This elasticity plane problem can be reduced to solving the biharmonic equation below in Terms of an Airy stress function (Sneddon and Berry, 1958):

$$\Delta^2 \Phi(x,y) = 0. \tag{1}$$

The stress and displacement's components can be expressed through the function $\Phi(x,y)$ as:

$$\sigma_y(x,y) = \frac{\partial^2 \Phi(x,y)}{\partial x^2}, \quad \sigma_x(x,y) = \frac{\partial^2 \Phi(x,y)}{\partial y^2},$$
$$\tau_{xy}(x,y) = -\frac{\partial^2 \Phi(x,y)}{\partial x \partial y}, \tag{2}$$

$$u_x(x,y) = \frac{1}{E}\left(\int \frac{\partial^2 \Phi(x,y)}{\partial y^2} dx - \nu \frac{\partial \Phi(x,y)}{\partial x} + U_0\right), \tag{3}$$

$$u_y(x,y) = \frac{1}{E}\left(\int \frac{\partial^2 \Phi(x,y)}{\partial x^2} dy - \nu \frac{\partial \Phi(x,y)}{\partial y} + V_0\right). \tag{4}$$

In the above

$$\Delta^2 = \frac{\partial^2}{\partial x^2} + \frac{\partial^2}{\partial y^2} \tag{5}$$

is the Laplace operator; E and ν are the Young's modulus and Poisson's ratio, respectively; and

U_0 and V_0 are constants. Eqs. (1)–(4) are valid for a plane stress problem. For a plane strain problem E and ν should be replaced by $E \to \frac{E}{1-\nu^2}$ and $\nu \to \frac{\nu}{1-\nu}$. To avoid confusion, the Airy stress function and the associated stress and displacement quantities for the regions above and below the crack plane will be denoted by a subscript "1" or "2". Specifically, the region above the crack plane $-\infty < x < \infty$, $0 < y \leqslant h_1$ will be assigned the subscript "1", and the region below the crack plane $-\infty < x < \infty$, $h_2 \leqslant y < 0$ will be assigned the subscript "2".

2.1. Boundary conditions

The boundary conditions will be written in the following form:

$$\sigma_y^{(j)}(\boldsymbol{x}, \boldsymbol{l_j}) = \boldsymbol{p_j}(\boldsymbol{x}), \quad \tau_{xy}^{(j)}(\boldsymbol{x}, \boldsymbol{l_j}) = 0, \quad -\infty \leqslant \boldsymbol{x} < \infty;$$
$$j = 1,2; \quad l_1 = h_1, \quad l_2 = -h_2, \tag{6}$$

$$\sigma_y^{(l)}(x,0) = \sigma_y^{(2)}(x,0), \quad \tau_{xy}^{(l)}(x,0) = \tau_{xy}^{(2)}(x,0),$$
$$u_y^{(l)}(x,0) = u_y^{(2)}(x,0), \quad -\infty \leqslant x < \infty, \tag{7}$$

$$\begin{cases} u_x^{(1)}(x,0) = u_x^{(2)}(x,0) & x_0 < |x| < \infty, \\ \tau_{xy}^{(1)}(x,0) = \tau_{xy}^{(2)}(x,0) = \tau(x) & -x_0 < x < x_0. \end{cases} \tag{8a,b}$$

In addition to (6), (7), (8a,b) we should add the overall equilibrium condition of the layer

$$\int_{-\infty}^{\infty} x^k p_1(x) d\lambda = \int_{-\infty}^{\infty} (-1)^k x^k p_2(x) d\lambda, \quad k = 0,1 \tag{9}$$

In (8) the function $\tau(x)$ represents the distribution of shear stress on the contacting crack surfaces. In this paper for $\tau(x)$ we will assume:

$$\tau(x) = \begin{cases} 0 & \textit{for frictionless contact between crack surfaces}, \\ k_0 \sigma_y(x,0) & \textit{for Coulomb friction between crack surfaces}, \\ \tau_0(x) & \textit{for adhesive friction with a known shear stress}. \end{cases} \tag{10}$$

where k_0 is a Coulomb friction coefficient.

In addition to the boundary conditions (6), (7) and (8a,b) we should add the condition $\sigma_y(x,\pm 0) < 0$.

When $-x_0 < x < x_0$. This condition is necessary for crack surfaces to be in full contact. Later we will show that depending on the location of applied external forces and on the geometry of the cracked layer the mentioned full contact condition may be violated.

3. Solution of the problem

The solutions of the bi-harmonic Eq. (1) can be represented by the following integral transforms for the regions "1" and "2" (Sneddon and Berry, 1958; Sneddon, 1955):

$$\Phi^{(j)}(x,y) = \int_{-\infty}^{\infty} [A_j(\lambda)\sinh\lambda y + B_j(\lambda)\lambda y\cosh\lambda y + C_j(\lambda)\cosh\lambda y + D_j(\lambda)\lambda y\sinh\lambda y]e^{-i\lambda x}d\lambda, \tag{11}$$

Using relations (2)–(4) and the representation (11), the stress and displacement components can be expressed as:

$$\sigma_y^{(j)}(x,y) = -\int_{-\infty}^{\infty} \lambda^2\{[B_j(\lambda)\lambda y + C_j(\lambda)]\cosh\lambda y + [D_j(\lambda)\lambda y + A_j(\lambda)]\sinh\lambda y\}e^{-i\lambda x}d\lambda, \tag{12}$$

$$\tau_{xy}^{(j)}(x,y) = i\int_{-\infty}^{\infty} \lambda^2\{[B_j(\lambda)\lambda y + C_j(\lambda) + D_j(\lambda)]\sinh\lambda y + [D_j(\lambda)\lambda y + A_j(\lambda) + B_j(\lambda)]\cosh\lambda y\}e^{-i\lambda x}d\lambda, \tag{13}$$

$$\sigma_x^{(j)}(x,y) = \int_{-\infty}^{\infty} \lambda^2\{[B_j(\lambda)\lambda y + C_j(\lambda) + 2D_j(\lambda)]\cosh\lambda y + [D_j(\lambda)\lambda y + A_j(\lambda) + 2B_j(\lambda)]\sinh\lambda y\}e^{-i\lambda x}d\lambda, \tag{14}$$

$$\frac{\partial u_x^{(j)}(x,y)}{\partial x} = \frac{1}{E}\int_{-\infty}^{\infty} \lambda^2\{[(1+\nu)(B_j(\lambda)\lambda y + C_j(\lambda)) + 2D_j(\lambda)] \times \cosh\lambda y + [(1+\nu)(D_j(\lambda)\lambda y + A_j(\lambda)) + 2B_j(\lambda)] \times \sinh\lambda y\}e^{-i\lambda x}d\lambda, \tag{15}$$

$$\frac{\partial u_y^{(j)}(x,y)}{\partial x} = \frac{i}{E}\int_{-\infty}^{\infty} \lambda^2\{[(1+\nu)(B_j(\lambda)\lambda y + C_j(\lambda)) - (1-\nu)D_j(\lambda)] \times \sinh\lambda y + +[(1+\nu)(D_j(\lambda)\lambda y + A_j(\lambda)) - (1 - \nu)B_j(\lambda)]\cosh\lambda y\}e^{-i\lambda x}d\lambda. \tag{16}$$

In the above, the functions

$$A_j(\lambda), \quad B_j(\lambda), \quad C_j(\lambda), \quad D_j(\lambda), \quad (\ j = 1,2) \tag{17}$$

are unknown and to be determined from the boundary conditions (6), (7) and (8a,b).

Before applying the boundary conditions 6,7,8a,b let us introduce a new unknown function

$$u(x) = \frac{\partial\left[u_x^{(1)}(x,0) - u_x^{(2)}(x,0)\right]}{\partial x}. \tag{18}$$

Using (18) the boundary condition (8a) will be replaced by

$$\frac{\partial[u_x^{(1)}(x,0) - u_x^{(2)}(x,0)]}{\partial x} = \begin{cases} u(x), & |x| < x_0, \\ 0, & |x| > x_0. \end{cases} \tag{19}$$

It is noted that $u(x)$ is unknown and must be determined from the (8b).

Based on the Fourier integral transformation technique

$$U(\lambda) = \frac{1}{2\pi}\int_{-x_0}^{x_0} u(x)e^{i\lambda x}dx, \quad P_j(\lambda) = \frac{1}{2\pi}\int_{-\infty}^{\infty} p_j(x)e^{i\lambda x}dx (j = 1,2) \tag{20}$$

from the boundary conditions (6), (7) and (19), we can get the following system of algebraic equations for the unknown functions (17):

$$[l_j\lambda B_j(\lambda) + C_j(\lambda)]\cosh l_j\lambda + [A_j(\lambda) + l_j\lambda D_j(\lambda)]\sinh l_j\lambda = -\lambda^{-2}P_j(\lambda)(j = 1,2,), \tag{21}$$

$$[A_j(\lambda) + B_j(\lambda) + l_j\lambda D_j(\lambda)]\cosh l_j\lambda + [C_j(\lambda) + D_j(\lambda) + l_j\lambda B_j(\lambda)]\sinh l_j\lambda = 0(j = 1,2,), \tag{22}$$

$$C_1(\lambda) - C_2(\lambda) = 0, \quad A_1(\lambda) + B_1(\lambda) - A_2(\lambda) - B_2(\lambda) = 0, \tag{23a, b}$$

$$(1+\nu)A_1(\lambda) - (1-\nu)B_1(\lambda) - (1+\nu)A_2(\lambda) + (1-\nu)B_2(\lambda) = 0, \tag{24}$$

$$(1+\nu)C_1(\lambda) + 2D_1(\lambda) - (1+\nu)C_2(\lambda) - 2D_2(\lambda) = E\lambda^{-2}U(\lambda). \tag{25}$$

The solution for the system of the Eqs. (21–25) are given by

$$A_1(\lambda) \equiv A_2(\lambda) = \frac{1}{2\Delta(\lambda)\lambda^2}\left\{-P_1(\lambda)\overline{P_1}(h_1\lambda,h_2\lambda) + P_2(\lambda)\overline{P_1}(h_1\lambda,h_2\lambda) + \frac{U(\lambda)\lambda^2}{2}\left[h_2^2\sinh 2h_1\lambda + 2h_1h_2(h_1+h_2)\lambda + h_1^2\sinh 2h_2\lambda\right]\right\}. \tag{26a, b}$$

$$B_1(\lambda) \equiv B_2(\lambda) = \frac{1}{2\Delta(\lambda)\lambda^2}\{P_1(\lambda)\overline{P}_1(h_1\lambda,h_2\lambda) - P_2(\lambda)\overline{P}_1(h_1\lambda,h_2\lambda) - \frac{U(\lambda)}{4}[-2h_1\lambda - 2h_2\lambda + 2h_2\lambda\cosh 2h_1\lambda + 2h_1\lambda\cosh 2h_2\lambda - \sinh 2h_1\lambda - \sinh 2h_2\lambda + \sinh 2(h_1+h_2)\lambda]\}, \tag{27a, b}$$

$$C_1(\lambda) \equiv C_2(\lambda) = \frac{1}{2\Delta(\lambda)\lambda^2}\left\{P_1(\lambda)\overline{P_3}(h_1\lambda,h_2\lambda) + P_2(\lambda)\overline{P_3}(h_1\lambda,h_2\lambda) - \frac{U(\lambda)\lambda^2}{2}[h_1^2(1-\cosh 2h_2\lambda) - h_2^2(1-\cosh 2h_1\lambda)]\right\},$$

$$D_2(\lambda) = D_1(\lambda) - \frac{EU(\lambda)}{2\lambda^2}, \tag{28a-c}$$

$$D_1(\lambda) = \frac{1}{2\Delta(\lambda)\lambda^2}\left\{P_1(\lambda)\overline{P_4}((h_1\lambda,h_2\lambda) + \frac{P_2(\lambda)}{2\Delta(\lambda)}\overline{P_4}((h_1\lambda,h_2\lambda) - \frac{U(\lambda)}{4}[1 + 4h_2(h_1+h_2)\lambda^2 + \cosh 2h_1\lambda - \cosh 2h_2\lambda - \cosh 2(h_1+h_2)\lambda - 2h_2\lambda\sinh 2h_1\lambda + 2h_1\lambda\sinh 2h_2\lambda]\right\}. \tag{29}$$

In the above expressions, the unknown functions (17) are represented in terms of the single unknown function $U(\lambda)$, which is the Fourier transform of the unknown function (18). Note that $u(x)$, thus $U(\lambda)$, will be determined such that the shear stress condition on the contacting crack surfaces (see (10) and the second condition in (8)) will be satisfied.

In (26–29) the following notations are used:

$$\overline{P_1}(h_1\lambda,h_2\lambda) = (h_1+2h_2)\lambda\cosh h_1\lambda + h_1\lambda\cosh(h_1+2h_2)\lambda + [1 + 2h_2(h_1+h_2)\lambda^2\sinh h_1\lambda] + \sinh(h_1+2h_2)\lambda, \tag{30}$$

$$\overline{P_2}(h_1\lambda,h_2\lambda) = \{2(h_1+h_2)\lambda\cosh h_1\lambda + \sinh h_1\lambda + \sinh(h_1+2h_2)\lambda\}, \tag{31}$$

$$\overline{P_3}(h_1\lambda,h_2\lambda) = (h_1+2h_2)\lambda\sinh h_1\lambda - h_1\lambda\sinh(h_1+2h_2)\lambda + [1 + 2h_2(h_1+h_2)\lambda^2\cosh h_1\lambda] - \cosh(h_1+2h_2)\lambda, \tag{32}$$

$$\overline{P_4}(h_1\lambda,h_2\lambda) = \{\cosh(h_1+2h_2)\lambda - \cosh h_1\lambda - 2(h_1+h_2)\lambda\sinh h_1\lambda\} \tag{33}$$

and the following non-dimensional parameters are introduced:

$$\frac{h_j}{x_0} \to h_i, \quad \frac{x}{x_0} \to x, \quad \frac{u(x)}{x_0} \to u(x), \quad \frac{p_j(x)}{x_0 E} \to p_j(x). \tag{34}$$

To determine $U(\lambda)$ the second condition in (8a,b) must be utilized. Inserting the functions from (17) into the expression for the shear stress (13) on the surface $y = 0$, we will get:

$$\begin{aligned}\frac{\tau_{xy}^{(1)}(x,0)}{E} &\equiv \frac{\tau_{xy}^{(2)}(x,0)}{E} \\ &= -\frac{i}{8}\int_{-\infty}^{\infty} U(\lambda)[2sgn(\lambda) + \psi(\lambda)]e^{-i\lambda x}d\lambda \\ &\quad + \frac{i}{2}M(x) \quad -\infty < x < \infty.\end{aligned} \tag{35}$$

In the Eq. (35)

$$\psi(\lambda) = \frac{\psi_1(\lambda)}{\Delta(\lambda)}, \quad M(x) = \int_{-\infty}^{\infty}\varphi(\lambda)e^{-i\lambda x}d\lambda, \quad \varphi(\lambda) = \frac{\varphi_{p1}(\lambda) + \varphi_{p2}(\lambda)}{\Delta(\lambda)}, \tag{36a-c}$$

$$\Delta(\lambda) = \sinh^2[\lambda(h_1 + h_2)] - [\lambda(h_1 + h_2)]^2, \tag{37}$$

$$\begin{aligned}\psi_1(\lambda) &= sgn(\lambda) + \frac{1}{2}[1 - sgn(\lambda)]e^{2(h_1+h_2)\lambda} - \frac{1}{2}[1 \\ &\quad + sgn(\lambda)]e^{-2(h_1+h_2)\lambda} - 2(h_1 \\ &\quad + h_2)\lambda\left[1 - (h_1 + h_2)\lambda sgn(\lambda) + 2h_1h_2\lambda^2\right] \\ &\quad - \left(1 + 2h_2^2\lambda^2\right)\sinh 2h_1\lambda - \left(1 + 2h_1^2\lambda^2\right)\sinh 2h_2\lambda \\ &\quad + 2h_2\lambda\cosh 2h_1\lambda + 2h_1\lambda\cosh 2h_2\lambda,\end{aligned} \tag{38}$$

$$\begin{aligned}\varphi_{p1}(\lambda) &= \lambda P_1(\lambda)\{h_1\cosh h_1\lambda - h_1\cosh(h_1 + 2h_2)\lambda \\ &\quad - 2h_2(h_1 + h_2)\lambda\sinh h_1\lambda],\end{aligned} \tag{39}$$

$$\begin{aligned}\varphi_{p2}(\lambda) &= -\lambda P_2(\lambda)[h_2\cosh h_2\lambda - h_2\cosh(h_2 + 2h_1)\lambda \\ &\quad - 2h_1(h_2 + h_1)\lambda\sinh h_2\lambda].\end{aligned} \tag{40}$$

By satisfying the shear stress condition in (8) we can get the following integral equation:

$$-\frac{i}{8}\int_{-\infty}^{\infty} U(\lambda)[2sgn(\lambda) + \psi(\lambda)]e^{-i\lambda x}d\lambda = -\frac{i}{2}M(x) + \tau(x) \quad -1 < x < 1, \tag{41}$$

Once this integral equation is solved, which will be done in the next section, the stress and displacement fields will be completely determined.

4. Solution of the integral equation (41)

In this section we will reduce the integral Eq. (41) to an infinite system of linear algebraic equations.

Two methods were developed for this purpose. The first method is described in the following paragraphs while the second method is briefly summarized in the Appendix.

4.1. Method 1: Chebyshev's orthogonal polynomials with a singular integral equation

Using the well-known integral (Prudnikov et al., 1998):

$$\int_{-\infty}^{\infty} sgn(\lambda)e^{-i(x-y)\lambda}d\lambda = -\frac{2i}{x-y}. \tag{42}$$

Eq. (41) can be reduced to following singular integral equation:

$$\begin{aligned}&-\frac{1}{4\pi}\int_{-1}^{1}\frac{u(y)}{x-y}dy - \frac{i}{16\pi}\int_{-1}^{1}u(y)dy\int_{-\infty}^{\infty}\psi(\lambda)e^{i\lambda(y-x)}d\lambda \\ &= -\frac{i}{2}M(x) + \tau(x) \quad -1 < x < 1.\end{aligned} \tag{43}$$

The integral Eq. (43) should be considered with the following condition

$$\begin{aligned}U(0) &= \frac{1}{2\pi}\int_{-1}^{1}u(x)dx = \frac{1}{2\pi}\int_{-1}^{1}[u_x^{(1)}(x,0) - u_x^{(2)}(x,0)]_{,x}dx \\ &= \frac{1}{2\pi}[u_x^{(1)}(x,0) - u_x^{(2)}(x,0)]\Big|_{x=-1}^{x=1} = 0,\end{aligned} \tag{44}$$

which can be derived from (18).

For the solution of the integral Eq. (43) we can use the Chebyshev's orthogonal polynomials method which is based on the following well-known spectral expression for the Chebyshev's orthogonal polynomials $T_m(x)$ (*first kind*) and $U_m(x)$ (*second kind*) (Prudnikov et al., 1998; Gradshtein and Ryzhik, 1994):

$$\frac{1}{\pi}\int_{-1}^{1}\frac{1}{x-y}\frac{T_m(y)}{\sqrt{1-x^2}}dy = -U_{m-1}(x), \quad m = 1,2,\ldots \tag{45}$$

Let us represent the solution of the integral Eq. (43) in the form of a series of the Chebyshev's orthogonal polynomials of the first kind (Klubin, 1969):

$$u(x) = \frac{1}{\sqrt{1-x^2}}\sum_{m=1}^{\infty}X_mT_m(x). \tag{46}$$

In (46) X_n (n = 1,2,...) are unknown coefficients that are to be determined. Let's note that the solution in the form of (46) automatically satisfies the condition (44). For completeness of the solution the summation in (46) should be started from "0". However, as shown below, the term with sub-index "0" is zero. Using the orthogonal conditions

$$\int_{-1}^{1}\frac{T_m(x)T_n(x)}{\sqrt{1-x^2}}dx = \begin{cases}0, & m = n, \\ \frac{\pi}{2}, & m = n \neq 0, \\ \pi, & m = n = 0\end{cases} \tag{47}$$

and the fact that $T_0(x) = 1$ we can derive:

$$\int_{-1}^{1}u(x)dx = \sum_{m=0}^{\infty}X_m\int_{-1}^{1}\frac{T_m(x)T_0(x)}{\sqrt{1-x^2}}dx = \pi X_0 = 0, \tag{48}$$

which means $X_0 = 0$.

Utilizing the well-known integral (Watson, 1995)

$$\int_{-1}^{1}\frac{T_m(x)e^{i\lambda x}}{\sqrt{1-x^2}}dx = (i)^m\pi J_m(\lambda), \tag{49}$$

the Fourier inverse transform $U(\lambda)$ of the function $u(x)$ can be expressed through the coefficients $X_n(n = 1,2,3\ldots)$ as follows:

$$U(\lambda) = \frac{1}{2\pi}\int_{-1}^{1}u(x)e^{i\lambda x}dx = \frac{1}{2}\sum_{m=1}^{\infty}(i)^mX_mJ_m(\lambda), \tag{50}$$

where the $J_m(\lambda)$, $(m = 1,2,\ldots)$ are the Bessel functions of the first kind.

Next we will continue to apply the Chebyshev's orthogonal polynomials method. To determine the remaining coefficients $X_n(n = 1,2,\ldots)$ we will substitute (46) into the (43) and use the spectral expression (45) to derive the following equation:

$$\begin{aligned}&\frac{1}{4}\sum_{m=1}^{\infty}X_mU_{m-1}(x) - \frac{i}{16}\sum_{m=1}^{\infty}(i)^mX_m\int_{-\infty}^{\infty}J_m(\lambda)\psi(\lambda)e^{-i\lambda x}d\lambda \\ &= -\frac{i}{2}M(x) + \tau(x), \quad -1 < x < 1.\end{aligned} \tag{51}$$

Using the following properties of Chebyshev's orthogonal polynomials of the second kind

$$\int_{-1}^{1}\sqrt{1-x^2}U_m(x)U_n(x)dx=\begin{cases}0, & m\neq n,\\ \frac{\pi}{2}, & m=n\end{cases} \tag{52}$$

and the known integral (Watson, 1995)

$$\int_{-1}^{1}\sqrt{1-x^2}U_{n-1}(x)e^{-i\lambda x}dx=(-i)^{n-1}\pi n\frac{J_n(\lambda)}{\lambda}, \tag{53}$$

finally we can get the following infinite system of linear algebraic equations for the unknown coefficients in the representation (46)

$$X_n+\sum_{m=1}^{\infty}A_{mn}X_m=a_n,\quad n=1,2,3,\ldots, \tag{54}$$

where

$$A_{mn}=\frac{n}{2}(-i)^n(i)^m\int_{-\infty}^{\infty}\lambda^{-1}\psi(\lambda)J_m(\lambda)J_n(\lambda)d\lambda\quad m,n=1,2,\ldots, \tag{55}$$

$$a_n=4n(-i)^n\int_{-\infty}^{\infty}\lambda^{-1}\varphi(\lambda)J_n(\lambda)d\lambda+\frac{8}{\pi}\int_{-1}^{1}\sqrt{1-x^2}U_{n-1}(x)\tau_0(x)dx. \tag{56}$$

4.2. Regularity of the infinite system of linear algebraic equations

The infinite system of linear algebraic Eq. (54) is quasi-regular if the following conditions hold (Kantorovich, 1964):

$$\lim_{n\to\infty}\sum_{m=1}^{\infty}|A_{mn}|=0,\quad \lim_{n\to\infty}a_n=0. \tag{57}$$

Note that the regularity of algebraic Eq. (54) strictly depends on behavior of functions $\psi(\lambda)$ and $\varphi(\lambda)$ when $\lambda\to\infty$. The function $\psi(\lambda)$ is infinitely time differentiable and exponentially tends to zero when $\lambda\to\infty$. That is, the function $\psi(\lambda)$ satisfies the inequality $\psi(\lambda)<M_0\,e^{-h\lambda}$, where $h=\min\{h_1,h_2\}$ and M_0 is some positive finite numbers. Using the above properties for $\psi(\lambda)$ and the inequality for Bessel functions (Watson, 1995)

$$|J_n(\lambda)|<\frac{\lambda^2}{n(n-1)},\quad \text{when } n>1, \tag{58}$$

we arrive at

$$|A_{mn}|=\left|\frac{n}{4}(i)^{m+n}\int_{-\infty}^{\infty}\lambda^{-1}\psi(\lambda)J_m(\lambda)J_n(\lambda)d\lambda\right|\leqslant M_{01}\frac{1}{(n-1)}\frac{1}{m(m-1)}. \tag{59}$$

When $n\to\infty$

$$\sum_{m=1}^{\infty}|A_{mn}|\to\frac{N_0}{(n-1)}+\frac{M_{01}}{(n-1)}\sum_{m=2}^{\infty}\frac{1}{m(m-1)}=\frac{M_{02}}{(n-1)}\to 0, \tag{60}$$

$$|a_n|=\left|4n(-i)^n\int_{-\infty}^{\infty}\lambda^{-1}\varphi(\lambda)J_n(\lambda)d\lambda+\frac{8}{\pi}\int_{-1}^{1}\sqrt{1-x^2}U_{n-1}(x)\tau_0(x)dx\right|\to\frac{M_{03}}{(n-1)}\to 0. \tag{61}$$

In (59)–(61) the coefficients $M_{0j}(j=1,2,3)$ are some positive finite constants.

5. Expressions for the normal and shear stresses along the line Y = 0 and the stress intensity factor (SIF)

Using the formulas (12), (13) and the representation (A1 and A2) we will have the following formulas for the shear and normal stresses along the line $y=0$:

$$\begin{aligned}\frac{\tau_{xy}^{(1)}(x,0)}{E}\equiv\frac{\tau_{xy}^{(2)}(x,0)}{E}&=-\frac{1}{8\sqrt{x^2-1}}\\&\times\sum_{m=1}^{\infty}\frac{(i)^mX_m\{[(-1)^m+1]\cos(m\pi/2)sgn(x)+i[(-1)^m-1]\sin(m\pi/2)\}}{\left(|x|+\sqrt{x^2-1}\right)^m}\\&-\frac{i}{16}\sum_{m=1}^{\infty}(i)^mX_m\int_{-\infty}^{\infty}\psi(\lambda)J_m(\lambda)e^{-i\lambda x}d\lambda+\frac{i}{2}M(x),\quad |x|>1,\end{aligned} \tag{62}$$

$$\begin{aligned}\frac{\sigma_y^{(1)}(x,0)}{E}\equiv\frac{\sigma_y^{(2)}(x,0)}{E}&=\frac{1}{4}\sum_{m=1}^{\infty}(i)^mX_m\int_{-\infty}^{\infty}\alpha(\lambda h_1,\lambda h_2)J_m(\lambda)e^{-i\lambda x}d\lambda\\&+\frac{1}{2}\int_{-\infty}^{\infty}[P_1(\lambda)\beta(\lambda h_1,\lambda h_2)+P_2(\lambda)\beta(\lambda h_2,\lambda h_1)]e^{-i\lambda x}d\lambda,\\&-\infty<x<\infty,\end{aligned} \tag{63}$$

where

$$\alpha(\lambda h_1,\lambda h_2)=\lambda^2(h_2^2\sinh^2\lambda h_1-h_1^2\sinh^2\lambda h_2)\Delta^{-1}(\lambda), \tag{64}$$

$$\begin{aligned}\beta(\lambda h_1,\lambda h_2)=\{&h_1\lambda\sinh(h_1+2h_2)\lambda-\left[1+2h_2\lambda^2(h_1+h_2)\right]\cosh h_1\lambda\\&+\cosh(h_1+2h_2)\lambda-(h_1+2h_2)\lambda\sinh h_1\lambda\}\Delta^{-1}(\lambda).\end{aligned} \tag{65}$$

From (62) and (63) it can be seen that the stress field has a mode II type singularity at the crack tips. Specifically, the shear stress has an inverse square-root singularity when $x\to\pm1$ and the normal stress σ_y is finite everywhere along y = 0 (even at the crack tips $\boldsymbol{x}=\pm1$). The mode II stress intensity factor (SIF) for the singular shear stress can be calculated in the following form:

$$\begin{aligned}K_{II}^{\pm}&=\lim_{x\to\pm1}\tau_{xy}(x,0)\sqrt{\pi|x^2-1|}\\&=-\frac{E\sqrt{\pi}}{8}\sum_{m=1}^{\infty}(i)^mX_m\{[(-1)^m+1]\cos(m\pi/2)sgn(x)\\&\quad+i[(-1)^m-1]\sin(m\pi/2)\},\\K_I^{\pm}&=\lim_{x\to\pm1}\sigma_y(x,0)\sqrt{\pi|x^2-1|}=0.\end{aligned} \tag{66a, b}$$

It will be not hard to estimate the angle of initial crack extension especially for discussed case. From (66a, b) we can see that intensity factor $K_I^{\pm}=0$ and $K_{II}^{\pm}\neq0$ from which is following that the initial crack extension direction should be along the crack line (perpendicular to the applied forces).

6. Numerical results

The regularity of the algebraic Eq. (54) can be seen numerically. However the required number of truncated system of equations strictly depends on the thickness of the layer and the locations of the applied external forces. For a moderately thick layer with $h_1\sim1$ and $h_2\sim1$ (note the non-dimensional normalizations introduced in (34)) the solutions of the truncated systems with $N=30$ equations and $N=20$ equations are different by $\sim10^{-4}$. In addition, when the number of equations in (55) N > 15 the coefficients X_n are on the order of 10^{-5}. For a very thin layer, i.e. $h_1+h_2<<1$, the solution of (54) converges slowly (the coefficients X_n will be on the order of 10^{-5} only when N > 50).

For numerical purposes we will consider the case of non-symmetric concentrated forces with $p_1(x) = -P_1[\delta(x-a_1) + \delta(x-b_1)]$ and $p_2(x) = -P_2[\delta(x-a_2) + \delta(x-b_2)]$, where a_i and b_i (i = 1,2) are the locations of the forces; P_i(i = 1,2) are the magnitudes of the concentrated forces, and $\delta(x)$ is the Dirac–Delta function. In particular, loading parameter values $P_1 = 1$, $P_2 = 2$, $a_1 = -5$, $a_2 = 0$, $b_1 = 15$, $b_2 = 5$, are used as an example. Note that the choice of these parameter values satisfies the overall equilibrium conditions specified in (9). The influence of various parameters (e.g. layer thickness) on the distributions of the normalized shear stress ($E^{-1}\tau_{xy}^{(1)}(x,0) \equiv E^{-1}\tau_{xy}^{(2)}(x,0)$) and the normalized normal stress ($E^{-1}\sigma_y^{(1)}(x,0) \equiv E^{-1}\sigma_y^{(2)}(x,0)$) will be described below. Concentrated forces coefficients and locations we choice in such a way as to get strong bending effect around crack location.

For the example described above, calculations have been carried out for the cases of (a) frictionless crack surface contact; (b) frictional crack surface contact with the Coulomb friction with a friction coefficient of $k_0 = 0.5$; and (c) adhesive friction with a known function $\tau_0(x) = 0.5(x-1)$ (for different type of friction laws see Gladwell, 1980). The bottom region thickness will be taken to be $h_2 = 5$ while the top region thickness h_1 will take values 2, 3, 4 and 5, and the effects of this thickness variation on the stress field and SIF will be evaluated.

Table 1 shows the influence of the top region thickness h_1 (and thus the total layer thickness) and the type of friction on the stress intensity factors $K_{II}^{+}/E\sqrt{\pi}$ (for the crack tip at $x = 1$) and $K_{II}^{-}/E\sqrt{\pi}$ (for the crack tip at $x = -1$). It is seen that, in the case of adhesive contact with the known shear stress function, the SIFs first increase quickly and then decrease quickly as h_1 increases from 2 to 3 and then to 5. In the cases of frictionless and Coulomb friction contact, several observations can be made. First, the overall trend is that the SIFs first almost remain constant and then decrease slowly as h_1 increases from 2 to 3 and then to 5. Second, the SIFs at the left and right crack tips have very similar values even though the loading is not very symmetrical about the midpoint between the crack tips. Third, it seems the SIFs are not strongly dependent on the friction coefficient value (the maximum difference is about 1∼ 2% between $k_0 = 0.0$ and $k_0 = 0.5$).

Detailed stress and strain variations along the crack line (the x axis) are shown in Figs. 2–9. For the singular shear stress, the stress distribution is shown only ahead of the right crack tip at $x = 1.0$.

6.1. Frictionless contact case

Fig. 2. shows the variation of the normalized shear stress $\tau_{xy}^{(1)}(x,0)/E$ with x ahead of the right crack tip (which is at $x = 1.0$), which indicates that the stress level is higher as the crack tip is approached, consistent with the existence of a shear stress singularity at the crack tip.

Fig. 3 shows the variation of the normalized normal stress $\sigma_y^{(1)}(x,0)/E$ along the x-axis. It is seen that the normal stress is finite along the entire x-axis (i.e. the normal stress has no singularity at the crack tips along the x-axis). It is also necessary to note that the normal stress becomes positive in the crack region (-1.0,1.0) for the case of the thickness parameter value $h_1 = 2$, which violates the crack surface contact condition (the normal stress must be negative in the crack region) and thus the solution for this particular case is not valid. For the other three thickness parameter values, the normal stress stays negative in the crack region and thus the solution is valid. This example demonstrates that the formulated problem requiring full crack surface contact under compressive loading may not be physically possible for certain parameter

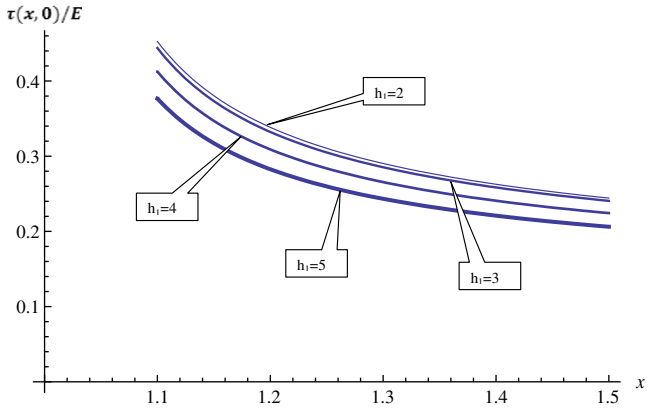

Fig. 2. Variation of $\tau_{xy}^{(1)}(x,0)/E$ with x ahead of the right crack tip for various values of h_1, for the frictionless contact case.

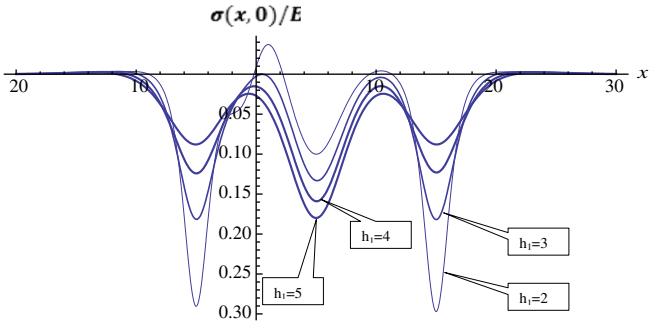

Fig. 3. Variation of $\sigma_y^{(1)}(x,0)/E$ along the x-axis for various values of h_1, for the case of frictionless crack surface contact.

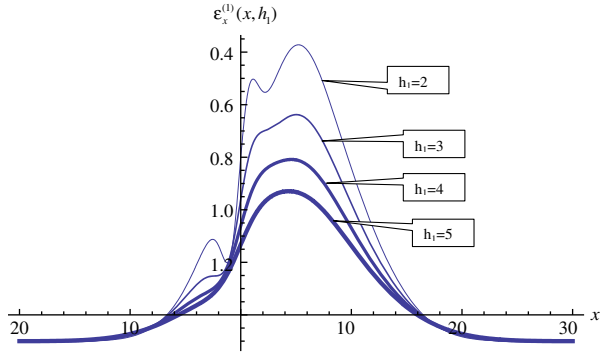

Fig. 4. Variation of $\varepsilon_x^{(1)}(x,h_1)$ with x on the top surface of a cracked layer for various values of h_1, for the case of frictionless crack surface contact.

Table 1
Values of stress intensity factors.

Coulomb friction ($k_0 = 0.5$)					Frictionless contact ($k_0 = 0.0$)				Adhesive friction ($\tau_0(x) = 0.5(x-1)$)			
h1:	2	3	4	5	2	3	4	5	2	3	4	5
$K_{II}^{+}/E\sqrt{\pi}$	0.187	0.190	0.184	0.175	0.189	0.186	0.173	0.157	0.469	3.281	1.761	1.102
$K_{II}^{-}/E\sqrt{\pi}$	0.191	0.193	0.184	0.171	0.190	0.189	0.176	0.158	0.973	3.331	1.810	1.131

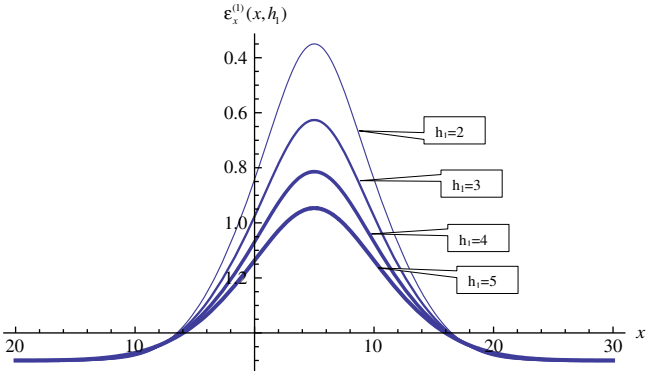

Fig. 5. Variation of $\varepsilon_x^{(1)}(x,h_1)$ with x on the top surface of a non-cracked layer for various values of h_1, for the case of frictionless crack surface contact.

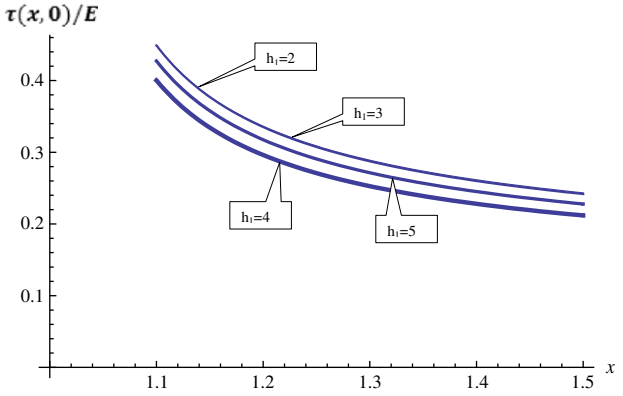

Fig. 6. Variation of $\tau_{xy}^{(1)}(x,0)/E$ with x ahead of the right crack tip for various values of h_1, for the case of frictional crack surface contact obeying the Coulomb friction law with a coefficient of $k_0 = 0.5$.

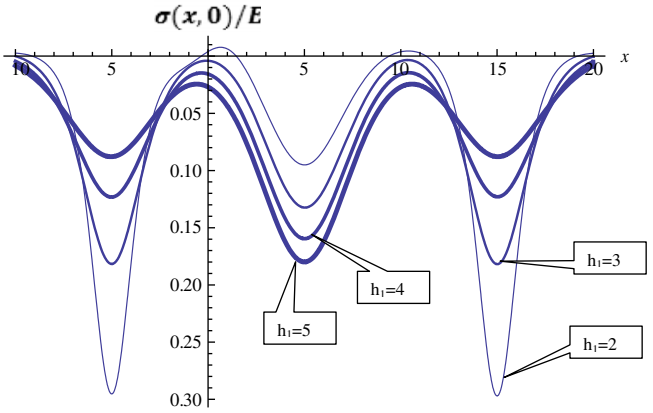

Fig. 7. Variation of $\sigma_y^{(1)}(x,0)/E$ along the x-axis for various values of of h_1, for the case of frictional crack surface contact obeying the Coulomb friction law with a coefficient of $k_0 = 0.5$.

values (e.g. for relatively thin layers, i.e. $h_1 + h_2 < 1$ and for certain locations of the external forces that lead to strong bending effects).

Figs. 4 and 5 respectively, show the variation of the longitudinal strain $\varepsilon_x^{(1)}(x,h_1)$ on the top surface of the layer in a cracked layer and a non-cracked layer for various h_1 values. These two figures provide a comparison of the distributions of the observable surface strain in a cracked layer and in a non-cracked layer and offer insights about the effect of the crack's presence on the strain distribution. In particular, it can be seen that the surface strain values in

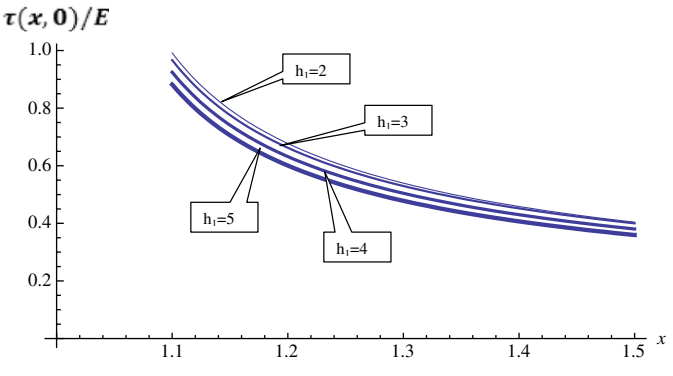

Fig. 8. Variation of $\tau_{xy}^{(1)}(x,0)/E$ with x ahead of the right crack tip for various values of h_1, for the case of frictional crack surface contact obeying an adhesive friction law with a known shear stress function $\tau_0(x) = 0.5(x-1)$.

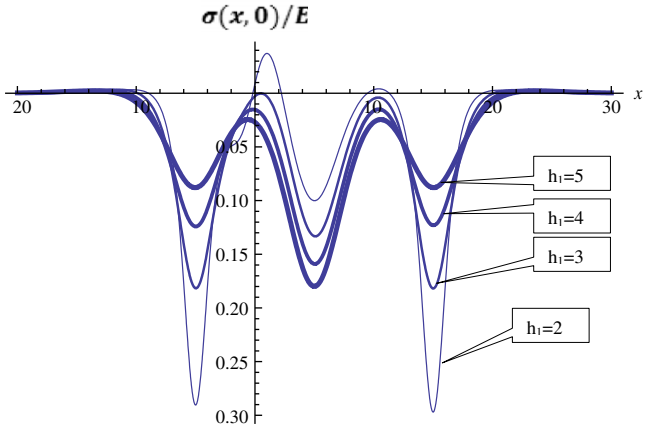

Fig. 9. Variation of $\sigma_y^{(1)}(x,0)/E$ along the x axis for various values of h_1, for the case of frictional crack surface contact obeying an adhesive friction law with a known shear stress function $\tau_0(x) = 0.5(x-1)$.

the cracked and non-cracked layers sometimes can be different by 40%.

6.2. Coulomb friction contact case

For the case of frictional crack surface contact obeying the Coulomb friction law with a friction coefficient of $k_0 = 0.5$, Fig. 6 shows the variation of the normalized shear stress $\tau_{xy}^{(1)}(x,0)/E$ with x ahead of the right crack tip (which is at $x = 1.0$), Fig. 7 shows the variation of the normalized normal stress $\sigma_y^{(1)}(x,0)/E$ with along the x-axis. The features of these variations are similar to those shown in Figs. 3 and 4 for the frictionless contact case, mainly that the shear stress variation indicates a stress singularity at the crack tip along the x-axis while the normal stress is finite along the entire x-axis. Also, the solution for the thickness value of $h_1 = 2$ shows a positive normal stress within the crack contact zone, which violates the full contact condition and thus the solution is invalid.

6.3. Adhesive friction contact case

For the case of frictional crack surface contact obeying an adhesive friction law with a known shear stress function $\tau_0(x) = 0.5(x-1)$, Fig. 8 shows the variation of the normalized shear stress $\tau_{xy}^{(1)}(x,0)/E$ with x ahead of the right crack tip (which is at $x = 1.0$), and Fig. 9 shows the variation of the normalized normal stress $\sigma_y^{(1)}(x,0)/E$ along the x axis. Again the main trend is similar to those shown in Figs. 3 and 4.

7. Conclusions

The boundary value problem of an elastic layer containing a finite length crack under compressive mechanical loadings has been studied. The crack surfaces are taken to be in full contact with frictionless contact or frictional contact with either the Coulomb friction law or an adhesive friction law.

Based on the Fourier integral transformation techniques the solution of the formulated problem is reduced to the solution of a singular integral equation, then, using the Chebyshev's orthogonal polynomials, to an infinite system of linear algebraic equations. The regularity of these equations is established. The expressions for the stress and displacement components in the elastic layer are presented. Based on the analytical solution, it is found that, along the x-axis (which aligns with the crack line) the shear stress has an inverse square root singularity at the crack tips while the normal stresses are finite.

Based on the developed analytical algorithm, extensive numerical investigations have been conducted. The results of these investigations are illustrated graphically exposing some novel qualitative and quantitative knowledge about stress concentration in the layer depending on some geometric and physical parameters of a layer. The numerical results show that the geometrical and physical parameters of the problem have an essential influence on the stress distribution around the crack. A stress distribution around crack surfaces in a case of frictional contact with the Coulomb friction law practically is similar to those in the case of frictionless contact. For example, even for large values of Coulomb friction coefficient (e.g. $k_0 \sim 0.8$) the differences between the shear stresses around the crack tip for a frictionless case and case with Coulomb friction law become no more than 3%. However there are quantitative and qualitative differences between the case with an adhesive friction law and the case of frictionless contact.

The findings of this study can serve as a theoretical basis for investigating stress concentration and crack growth in cracked material layers under compressive loading conditions.

Appendix A. Method 2: Chebyshev's orthogonal polynomials without a singular integral equation

Representation (50) can help us to propose another way to determine $U(\lambda)$ directly from (41) without going through the singular integral Eq. (43). Taking into account the following well-known integrals (Watson, 1995):

$$\int_{-\infty}^{\infty} sgn(\lambda)\lambda^{-1}J_n(\lambda)J_m(\lambda)d\lambda = \begin{cases} \frac{1}{n}, & n = m, \\ 0, & n \neq m, \end{cases} \tag{A1}$$

$$\int_{-\infty}^{\infty} sgn(\lambda)J_n(\lambda)e^{-i\lambda x}d\lambda = \begin{cases} 2(-i)^{n-1}U_{n-1}(x), & |x| < 1, \\ \frac{[(-1)^n-1]\sin\frac{n\pi}{2} - i[(-1)^n+1]\cos(n\pi/2)sgn(x)}{\sqrt{x^2-1}\left(|x|+\sqrt{x^2-1}\right)^n} & |x| > 1 \end{cases}, \tag{A2}$$

and substituting (50) into the (41) we can arrive at exactly the same linear algebraic Eq. (54). Note that this second method is a direct method for deriving the linear algebraic Eq. (54), without dealing with the singular integral Eq. (43).

The set of infinite number of linear algebraic Eq. (54) can be solved by the method of truncation to a set of finite number of linear algebraic equations. However, in order to apply the truncation method, we need to show the regularity of (54). Another approximate method for solving the singular integral Eq. (43) was proposed by Erdogan et al. (1973).

References

Bilby, B.A., Cardew, G.E., 1975. The crack with a kinked tip. Int. J. Fract. 11, 708–712.
Broberg, K.B., 1987. On crack paths. Eng. Fract. Mech. 28, 663–679.
Broberg, K.B., 1999. Cracks and Fracture. Academic Press, London, UK.
Civelek, M.B., Erdogan, F., 1974. The axisymmetric double contact problem for a frictionless elastic layer. Int. J. Solids Struct. 10 (6), 639–659.
Cotterell, B., Rice, J.R., 1980. Slightly curved or kinked cracks. Int. J. Fract. 16, 155–169.
Deng, X., 1993. General crack-tip fields for stationary and steadily growing interface cracks in anisotropic bimaterials. ASME J. Appl. Mech. 60, 183–188.
Deng, X., 1995. Mechanics of debonding and delamination in composites: asymptotic studies. Compos. Eng. 5, 1299–1315.
Dhirendra, V.K., Narasimhan, R., 1998. Mixed-mode steady-state crack growth in elastic–plastic solids. Eng. Fract. Mech. 59, 543–559.
El-Borgi, S., Keer, L., Ben Said, W., 2004. An embedded crack in a functionally graded coating bonded to a homogeneous substrate under frictional Hertzian contact, wear. Int. J. Sci. Technol. Frict. Lubricat. Wear 257 (7–8), 760–776.
El-Borgi, S., Abdelmoula, R., Keer, L., 2006. A receding contact plane problem between a functionally graded layer and a homogeneous substrate. Int. J. Solids Struct. 43, 658–674.
Erdogan, F., Sih, G.C., 1963. On the crack extension in plates under plane loading and transverse shear. J. Basic Eng. 85, 519–525.
Erdogan, G.D., Gupta, T.S., Cook, T.S., 1973. The numerical solutions of singular integral equations. In: Method of Analysis and Solutions of Crack Problems. Noordhoff International Publishing, Leyden, pp. 268–425.
Ghonem, H., Kalousek, J., 1988. Study of surface crack initiation due to biaxial compression/shear loading. Eng. Fract. Mech. 30, 667–683.
Gladwell, G.M.L., 1980. Contact Problems in the Classical Theory of Elasticity. Sijthoff & Noordhoff International Publishers B.V. p. 705.
Gradshtein, I.S., Ryzhik, I.M., 1994. Tables of Integrals. Sums, Fifth ed.. Sums, Series and Products Academic Press.
Hallbfack, N., 1998. Mixed mode I/II fracture behaviour of a high strength steel. Int. J. Fract. 87, 363–388.
Hammouda, M.M.I., Fayed, A.S., Sallam, H.E.M., 2002. Mode II stress intensity factors for central slant cracks with frictional surfaces in uniaxially compressed plates. Int. J. Fatigue 24, 1213–1222.
Hancock, W., 1999. Mode I and mixed-mode fields with incomplete crack-tip plasticity. Int. J. Solids Struct. 36, 711–725.
Hayashi, K., Nemat-Nasser, S., 1981. On branched, interface cracks. ASME J. Appl. Mech. 48, 529–533.
Hearle, A.D., Johnson, K.L., 1985. Mode II stress intensity factors for a crack parallel to the surface of an elastic half-space subjected to a moving point load. J. Mech. Phys. Solids 33, 61–81.
Hill, R., 1950. The Mathematical Theory of Plasticity. Clarendon Press, Oxford, UK.
Hutchinson, J.W., 1968. Plastic stress and strain fields at a crack-tip. J. Mech. Phys. Sol. 16, 337–347.
Isaksson, P., Stahle, P., 2002. Mode II crack paths under compression in brittle solids—a theory and experimental comparison. Int. J. Solids Struct. 39, 2281–2297.
Isaksson, P., Stahle, P., 2003. A directional crack path criterion for crack growth in ductile materials subjected to shear and compressive loading under plane strain conditions. Int. J. Solids Struct. 40, 3523–3536.
Ishida, M., Abe, N., 1996. Experimental study on rolling contact fatigue from the aspect of residual stress. Wear 191, 65–71.
Jayaraman, S., Sadeghipour, K., Baran, G., 1997. Finite element analysis of horizontal and branched subsurface cracks in brittle materials. Wear 208, 237–242.
Kantorovich, L.N., 1964. Approximate Methods of Higher Analysis. Noordhoff LTD.
Keer, L.M., Dundurs, J., Tasi, K.C., 1972. Problems involving a receding contact between a layer and a half-space. J. Appl. Mech. 39, 1115–1120.
Klubin, P.I., 1969. Distribution of contact pressures between a plate with a base that is not flat and an elastic half-plane. Soil Mech. Found. Eng. (5), 10–12.
Komvopoulos, K., Cho, S.-S., 1997. Finite element analysis of subsurface crack propagation in a half-space due to a moving asperity contact. Wear 209, 57–68.
Lazarus, V., Buchholz, F.-G., Fulland, M., Wiebesiek, J., 2008. Comparison of predictions by mode II or mode III criteria on crack front twisting in three or four point bending experiments. Int. J. Fract. 153, 141–151.
Liu, A.F., 1974. Crack growth failure of aluminum plate under in-plane shear. AIAA J. 12, 180–185.
Makaryan, S., 2006, Behaviour of the crack under the compressing load, National Academy of Science of Armenia, In: Proceedings, vol 106, N2, Yerevan, pp 144–152.
Makaryan V., Sutton M., Yeghiazaryan T., Hasanyan D., Deng X., '2009'Cracked Elastic Half Plane Under a Compressive Mechanical Load'', 2009 ASME International Mechanical Engineering Congress & Exposition, Lake Buena Vista, Florida. November, pp. 13–19.
Melin, S., 1986. When does a crack grow under mode II conditions? Int. J. Fract. 30, 103–114.
Melin, S., 1987. Fracture from a straight crack subjected to mixed-mode loading. Int. J. Fract. 32, 257–263.
Prudnikov, A.P., Brichkov, Y.A., Marichev, O.I., 1998. Integrals and Series, vol. 2. Gordon & Beach Science Publishers.
Roy, Arun, Narasimhan, R., Arora, P.R., 1999. An experimental investigation of constraint effects on mixed mode fracture initiation in a ductile aluminum alloy. Acta Mater. 47, 1587–1596.

Sih, G.C., Williams, M.L., Swedlow, J.L., 1966. Three dimensional stress distribution near a sharp crack in a plate of finite thickness, AFML. Wright-Patterson Air Force Base, AFML-TR-66-242.

Sneddon I., 1955, Transformation of Fourier. Edition of foreign literature. Moscow.

Sneddon, I., Berry, M., 1958. The classical theory of elasticity. In: Flugge, S. (Ed.), Encycl. Phys. Elasticity and Plasticity, vol. VI. Springer-Verlag, Berlin, New York.

Sundara Raja Iyengar, K.T., Murthy, M.V.V., Bapu Rao, M.N., 1988. Three dimensional elastic analyses of cracked thick plates under bending fields. Int. J. Solids Struct. 24, 683–703.

Watson, G.N., 1995. A Treatise on the Theory of Bessel Functions, Second Edition, Cambridge University Press. OF DEBOND1NG AND DELAMINATION IN.

Wong, S.L., Bold, P.E., Brown, M.W., Allen, R.J., 1996. A branch criterion for shallow angled rolling contact fatigue cracks in rails. Wear 191, 45–53.